Chemistry Europe

AWARD

Nominate a Worthy Chemist Chemistry Europe Award

Subject:
chemistry for sustainability, energy, materials, environment

Consists of:
prize money amounting to EUR 10,000, certificate

Deadline:
November 1, 2022

Click here for more info & nomination

Minireviews
doi.org/10.1002/cplu.202100191

Chemistry Europe
European Chemical Societies Publishing

Special Collection

Germanium-Based Halide Perovskites: Materials, Properties, and Applications

Rossella Chiara, Marta Morana, and Lorenzo Malavasi*[a]

Perovskites are attracting an increasing interest in the wide community of photovoltaics, optoelectronic, and detection, traditionally relying on lead-based systems. This Minireview provides an overview of the current status of experimental and computational results available on Ge-containing 3D and low-dimensional halide perovskites. While stability issues analogous to those of tin-based materials are present, some strategies to afford this problem in Ge metal halide perovskites (MHPs) for photovoltaics have already been identified and successfully employed, reaching efficiencies of solar devices greater than 7% at up to 500 h of illumination. Interestingly, some Ge-containing MHPs showed promising nonlinear optical responses as well as quite broad emissions, which are worthy of further investigation starting from the basic materials chemistry perspective, where a large space for properties modulation through compositions/alloying/fnanostructuring is present.

1. Introduction

The use of metal halide perovskites (MHPs) in photovoltaics has grown in an impressive way in the last decade, providing, in recent times, certified power conversion efficiencies (PCEs) above 25%.[1] On the other hand, all the MHPs employed so far to achieve such high PCEs contain lead, and it is hard to believe that such technology will be used at large scale, particularly in Europe where stringent "lead free directives" are applied.[2] Therefore, in the last years, a huge interest is directed towards lead-free perovskites containing other metals such as Sn, Bi, Sb and Ge. As a result of these efforts, Sn-containing materials have been used with success in Perovskite Solar Cells (PSCs) with the actual highest efficiency results surpassing 13%, making Sn-based perovskites the most appealing materials for lead-free PSCs.[3] Sb and Bi containing phases are object of intense current investigation demonstrating relevant applications in the field of photodetectors and photocatalysis rather than photovoltaics.[4] Germanium-based MHPs are still scarcely investigated but we may anticipate a growing interest towards such materials in the next years for a wide spectrum of applications. Ge is an abundant metal and, with respect to lead, has little toxicity and environmental concerns. This allows to overcome a major drawback of Pb-containing perovskites but, on the other hand, germanium (present in MHPs as Ge^{2+}) shares with Sn^{2+} a strong tendency towards oxidation under ambient conditions. Advantageously, it can be anticipated that several stabilization routes applied to Sn-based perovskites to protect them from oxidation will work also for the Ge-containing counterparts.

In this Minireview we provide a snapshot of the current status of the research on Ge-based perovskites by organizing the paper according to the crystal structure of the materials investigated so far.

[a] R. Chiara, Dr. M. Morana, Prof. L. Malavasi
Department of Chemistry
University of Pavia and INSTM
Via Taramelli 16, 27100 Pavia > (Italy)
E-mail: lorenzo.malavasi@unipv.it

This article is part of a Special Collection on "Perovskite Materials and Devices"

2. Germanium Halide Perovskites

2.1. 3D perovskites

Hybrid organic-inorganic 3D germanium halide perovskites have been among the first to be deeply investigated in analogy with the Pb-containing materials. Stoumpos *et al.* reported in 2015 a series of $AGeI_3$ materials with A = methylammonium (MA), formamidinium (FO), acetamidinium (MFO), guanidinium, trimethylammonium, and isopropylammonium.[5] Only with the first three organic cations 3D perovskites where crystallized while, in the remaining cases, 1D infinite chains compounds were found, as also observed in analogous Pb-containing systems when the size of the organic cation increases.[6] For the 3D perovskite materials, Figure 1a shows the optical absorbance spectra including $CsGeI_3$ as reference compound. The band gap has been shown to increase progressively by 0.3 eV by replacing smaller Cs^+ cation with bigger MA (1.9 eV), FO (2.2 eV), and MFO (2.5 eV) cations.[5] This is a quite unusual trend since the organic cation size in Pb-based 3D perovskite only marginally affects the band gap. The increased spatial separation of the $[GeI_3]^-$ inorganic units induced by cation size is believed to be responsible for a reduced orbital overlap. This in

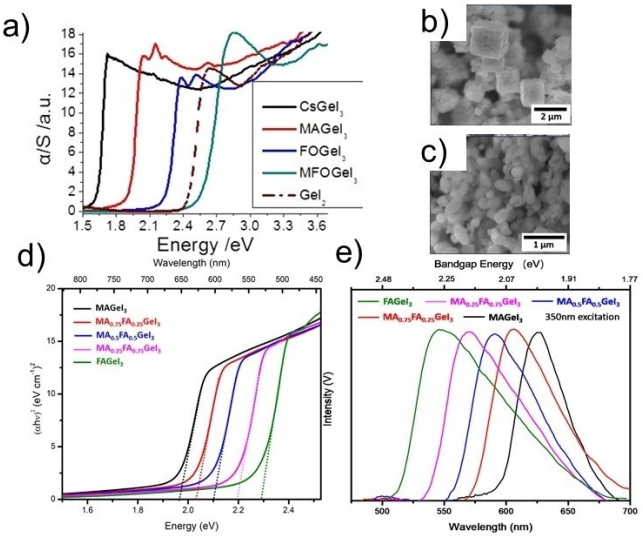

Figure 1. a) Absorption spectra of $AGeI_3$ 3D compounds where MA = methylammonium, FO = formamidinium, MFO = acetamidinium. Reproduced from reference [5] with permission from the American Chemical Society. b) SEM image of $MAGeI_3$ and c) of $FAGeI_3$; d) Tauc plots and e) PL spectra of the $MA1_{-x}FA_xGeI3$ (x = 0, 0.25, 0.5, 0.75, 1) solid solution. Reproduced from reference [7] with permission from Elsevier.

turn results in narrow bandwidths leading to a greater band separation and band gap increase.[5] The sharp absorption edges (Figure 1a) suggest a direct band gap which has been confirmed by theoretical calculations.[5] These materials were further subjected to Second Harmonic Generation (SHG) investigation. Main finding was the observation of SHG responses for $MAGeI_3$ and $FOGeI_3$ higher than best performing Ge-halide SHG material such as $CsGeI_3$. Experimental and theoretical investigation related this effect to the polarity of the cations employed.[5] Clearly, enlarging the family of hybrid organic-inorganic geranium halide perovskite could provide more solid conclusions regarding the role of A-site cation on nonlinear optical properties and help in designing even more efficient phases. Noteworthy, the recent emergence of chiral perovskites as suitable materials for nonlinear optical properties, among which SHG response, could be further explored by considering Ge-containing systems.[7]

More recently, the MA1–xFAxGeI3 (x = 0, 0.25, 0.5, 0.75, 1) solid solution was systematically investigated by Yue *et al.*[8] Differently from ref. 5, the authors devised a simple synthetic procedure modifying and adapting traditional ligand-assisted reprecipitation method for Pb-based perovskite synthesis, thus avoiding the use of concentrated HI and H_3PO_2.[8] X-ray Diffraction (XRD) study of the prepared samples confirmed phase pure materials with a progressive increase of the trigonal unit cell by increasing the amount of bigger FA. Scanning Electron Microscopy (SEM) yielded composition-dependent morphologies in terms of size and shape and representative images for MAGeI3 and FAGeI3 are reported in Figure 1b and 1c, respectively.[8] The optical properties characterization showed a progressive modulation of the band gap and emission spectra in the MA1–xFAxGeI3 (x = 0, 0.25, 0.5, 0.75, 1) solid solution, spanning the interval from 2.26 to 1.98 eV, with the values for the two end members in good agreement with the data reported in ref. 5. The Tauc plots and the normalized photoluminescence (PL) spectra of the samples investigated in ref. 7 are reported in Figures 1d and 1e, respectively. A progressive broadening of the PL spectra can be seen as a function of × (amount of FA) Interestingly, the analogous Pb-based system, namely MA1–xFAxPbI3, shows a very limited variation of the band gap moving from $MAPbI_3$ (1.48 eV) to $FAPbI_3$ (1.53 eV).[9] A clear definition of the stronger impact of the organic cation on Ge-based perovskites with respect to the Pb-analogues warrant further detailed structural investigation, e.g. by local structural probes, since this large effect may be exploited for electronic properties tuning as an additional degree of freedom with respect to halide substitution.[10–12]

The authors of ref. 7 carried out also a deep study on the stability of the prepared phase by performing XRD analysis as a function of exposure time of the perovskite under glove-box conditions and air. In general, while a good stability under argon storage has been found, air-exposure leads to GeO_2 formation after 24 hours, thus confirming the instability of the Ge^{2+} ion toward oxidation to Ge^{4+}.[8]

One of the first attempts to include Ge-based halide perovskites in PSCs dates back to 2015.[13] In particular, after computationally screening a series of possible candidates, Krishnamoorthy *et al.* prepared solar cells with the germanium iodide perovskites ($MAGeI_3$ and $CsGeI_3$) using compact and mesoporous TiO_2 as electron transport layer (ETL) and Spiro-OMeTAD as hole transport layer (HTL), respectively. In general, dissolution of germanium perovskite is difficult in most organic polar solvents, and bad morphologies are obtained, which impact the device performances.[13] In ref. 8, for example, $FAGeI_3$ could be deposited by spin-coating only with poor film quality which led to the impossibility of recording any photocurrent. For the PCSs based on $MAGeI_3$ and $CsGeI_3$ device efficiencies (PCEs) of 0.11% and 0.20% were obtained, respectively. More recently, Kopacic and co-workers investigated the photovoltaic performance of $MAGeX_3$ (X=I, Br) and observed that the perovskite becomes less prone to degradation by halide mixing with an improvement of the performance in solar cells.[14] In ref. 9 the germanium halide perovskites of formula $MAGeI_3$ (band gap 2.0 eV) and $MAGeI_{2.7}Br_{0.3}$ (band gap 2.1 eV) were

Lorenzo Malavasi is Associate Professor at the Chemistry Department of the University of Pavia and member of the INSTM Consortium. He is working in several areas of materials chemistry with particular interest in the investigation of structure-properties correlation in functional materials for sustainable and clean energy, in particular metal halide perovskites, and catalysis materials. He leads the Materials Chemistry Group at University of Pavia.

Marta Morana is Postdoctoral Fellow in the Material Chemistry Group at the Chemistry Department of the University of Pavia. Her research interests focus on structural characterization of materials by means of single crystal and powder X-ray diffraction, structure-properties correlation, and crystallography at high pressure.

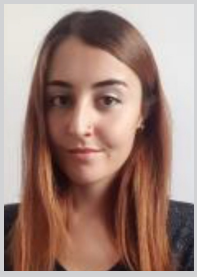

Rossella Chiara is a PhD student in the Materials Chemistry Group at the Chemistry Department of the University of Pavia. She is carring out her research activity in the field of low-dimensional lead-free hybrid perovskites.

prepared starting from GeI_2, MAI, and MABr, with dimethylformamide as solvent. The solution was spin coated (with a step of antisolvent dripping) and the film annealed at 70 °C for 10 min to obtain the film of the perovskite.[14] By means of time-resolved UV-vis spectroscopy, the authors verified the stability under ambient conditions of $MAGeI_3$ and $MAGeI_{2.7}Br_{0.3}$, with the latter film composition retaining the 65% of its initial absorption at 510 nm after 24 hours, relative to 32% of $MAGeI_3$.[14] Such improved ambient stability of the mixed $MAGeI_{2.7}Br_{0.3}$ was correlated to the lifetimes of the prepared PSCs. As a matter of fact, the solar cells based on $MAGeI_3$, even under inert conditions, lost their performance within few hours, while the mixed halide composition degradation was retarded, in analogy with lead-based counterparts PSCs.[15] The PSCs were assembled in the "organic" p–i–n solar cell architecture employing, as HTL, PEDOT:PSS and $PC_{70}BM$ as ETL, and their performance were studied as a function of the bromide content.[14] The results of the device performance are reported in Figure 2, showing a continuous increase of the photovoltage by increasing the Br-amount as a result of the increase of the band gap value. According to the data reported in ref. 9, the PCEs of the solar cells progressively increase up to a bromide content of 10%, displaying mean values quite constant around 0.45%.

Based on these results, the $MAGeI_{2.7}Br_{0.3}$ compositions was further optimized to improve the performance of the device by varying the thicknesses of PEDOT:PSS, $MAGeI_{2.7}Br_{0.3}$ and $PC_{70}BM$ ETL, leading to an improved PCE of 0.57%.[14] Such value reduced quickly to 0.21% within several hours after preparation, evidencing the known the stability issue of the Ge-based PSCs. Possibly, most of the strategies employed more recently for both Pb- and Sn-based PSCs could be profitably used to improve the stability of Ge-based cells such as by the used of additives and/or protective layers and 2D/3D configurations. In addition, the exploration of devices based on mixed $Ma/FAGeI_3$ and even triple cation configurations, together with mixed halides, could provide an improvement in cell stability and performances. Clearly, tailored HTM materials for such PSCs should developed.

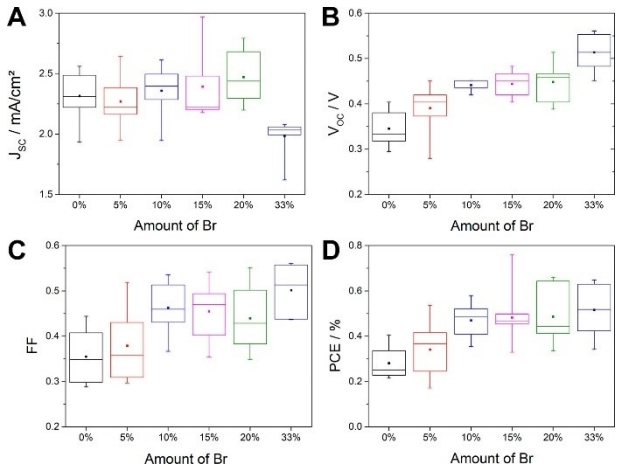

Figure 2. Characteristic parameters (A, J_{SC}; B, V_{OC}; C, FF; D, PCE) of the prepared solar cells depending on the amount of Br as X-site anion in $MAGeX_3$ (X=I, Br). Reproduced from reference [8] with permission from the American Chemical Society.

In parallel to these limited experimental works, advanced computational modelling has been used to explore the electronic and optical properties of Ge-containing perovskites, define their stability, and predict possible novel compositions. Sun and co-workers systematically studied the properties of $MAGeX_3$ perovskites in the trigonal phase (*R*3 *m* space group) by comparing them to the Pb and Sn-based perovskites with tetragonal phase (*I*4/*mcm*).[16] Structures and formation energies, electronic band-structures, and optical properties were calculated in great detail indicating, as main conclusions, that $MAGeI_3$ exhibits an electronic character close to the one of $MAPbI_3$ and that Ge-based perovskites are less prone to oxidation with respect to the Sn counterparts providing the following order of stability $MAPbI_3 > MAGeI_3 > MASnI_3$.[16] Interestingly, $MAGeI_3$ has been also computationally investigated for possible ferroelectricity.[17] Density Functional Theory (DFT) calculations revealed that $MAGeI_3$ exhibits strong ferroelectric polarization (~13.8 $\mu C\,cm^{-2}$ which has been correlated to strong GeI_6^- octahedra distortion on the **c**-axis. The relevant distortion induced by Ge on the octahedra framework seems to be a general properties of 3D and 2D (see later) Ge perovskites which should be further investigated to highlight symmetry-break induced properties. The system is mainly electron-dominated and demonstrates high absorption and transport anisotropy. Moreover, by tuning the ferroelectric polarization, an improvement of light absorption was calculated, which has been correlated to the increased p–p-orbital transitions. A possible increase of incident photon conversion efficiency has been related to a stronger ferroelectric polarization in $MAGeI_3$ which is beneficial for photovoltaic applications.[17] Recently, a revision of the electronic structure calculation of $MAGeI_3$ has been provided by Umadewi and Watson, in order to shed light on the discrepancies on the band gap values reported so far.[18] The authors applied range of theoretical methods confirming the direct nature of the MAGeI3 band gap, while the density-of-states (DOS) analysis indicates that the valence band is predominantly made up of I(p) states and the conduction band consists primarily of Ge(p) states.[18] Moreover, an agreement between the DOS characteristics and charge carrier effective masses between MAGeI3 and $MAPbI_3$ was reported.[18]

Finally, numerical simulations of PCS performances based on MAGeI3 have been reported by Kanoun and co-workers, with the aim of providing a guide to improve the Ge-based perovskite device efficiency.[19] The authors investigated the effect of absorber thickness, defect density, hole mobility, operating temperature, and metal work function of PCSs based on $MAGeI_3$.[19] Optimal absorber thickness ranges from 600 to 700 nm with the best calculated performance (>20%) reached for a PSC using Cu_2O and D-PBTTT-14 as HTM layers and Pt as back contact electrode.[19]

As for other 3D MHPs, B-site metal alloying has been explored also for Ge-based perovskites. A detailed experimental study on the $MASn_{1-x}Ge_xI_3$ ($0 \le x \le 1$) solid solution has been provided by Nagane *et al.* based also on the computational prediction of the possibility of realizing mixed Sn–Ge

perovskites.[20,21] From a structural point of view, the trigonal crystal structure of MAGeI3 is found up to $x = 0.75$, while for the other intermediate compositions the tetragonal structure (space group *P*4 *mm*, no. 99) of MASnI3 is observed, as reported in Figure 3a for powder samples. *Ab-initio* simulations confirmed the stability, under inert gas at 300 K, for all the mixed compositions indicating a favorable energetic stability of these materials in the perovskite phase.[20] The optical properties of $MASn_{1-x}Ge_xI_3$ ($0 \leq x \leq 1$) perovskite thin films fabricated on quartz substrates revealed a monotonic blue-shift of the band gap by increasing the Ge-content, as shown in Figure 3b, from about 1.3 eV for MASnI3 to about 1.9 eV for MAGeI3.[20] Moreover, at 50% Ge doping in MASnI3, the authors observed an amplified spontaneous emission (ASE) and the lowest disorder (Urbach energy of ~47 meV) among the entire family. This result, together with the band gap of ~1.5 eV for $MASn_{0.50}Ge_{0.50}I_3$, suggests that this composition could be ideal and further exploited in the fabrication an efficient single junction solar cells.[20]

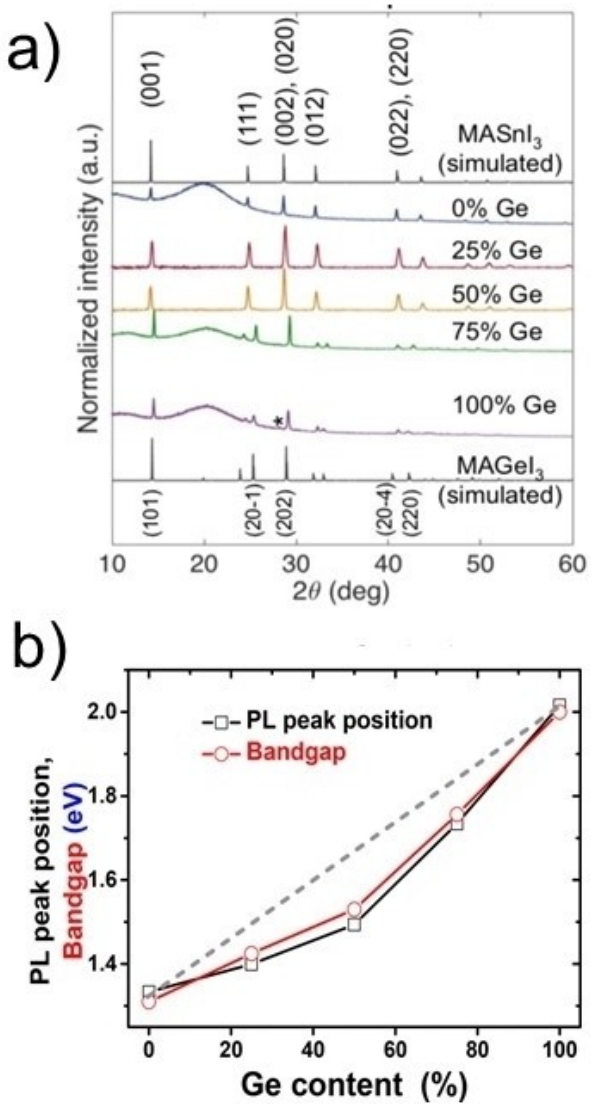

Figure 3. a) XRD patterns for 0% Ge ($MASnI_3$), 25% Ge ($MASn_{0.75}Ge_{0.25}I_3$), 50% Ge ($MASn_{0.50}Ge_{0.50}I_3$), 75% Ge ($MASn_{0.25}Ge_{0.75}I_3$), and 100% Ge ($MAGeI_3$) powder samples (* indicates small impurity phases.); b) Comparison of PL peak position and band gap of Sn–Ge perovskites as a function of Ge content (0 to 100%). Reproduced from reference [20] with permission from the American Chemical Society.

Indeed, a similar composition in terms of B-site cation has been shown to provide highly stable PSCs by Chen and co-workers.[22] The authors prepared the $CsSn_{0.5}Ge_{0.5}I_3$ perovskite by thermal evaporation in the form of thin films of average thickness around 200 nm. Such approach yielded very uniform, and ultrasmooth films (mean-square roughness around 2 nm) with a full coverage of the substrate.[22] Band gap of $CsSn_{0.5}Ge_{0.5}I_3$ is centered around 1.50 eV in agreement with computational studies.[21] One of the most striking result of this work was the observation of an impressive phase stability of the films after exposure to ambient atmosphere up to 24 hours, differently from the two parent compounds, namely $CsSnI_3$ and $CsGeI_3$. Such stability was also confirmed under continuous illumination (1-sun) in ambient atmosphere up to 72 h.[22] The origin of this superior stability was investigated by X-ray Photoelectron Spectroscopy (XPS) and was attributed to the formation, on the perovskite film, of a native-oxide layer comprising GeO_2 doped with a small portion of Sn. The authors made use of such improved stability to fabricate a solar cell using PCBM as ETL and spiro-OMeTAD as HTL layer. The native oxide layer served has a wide-bandgap interfacial layer between the perovskite and the HTL. A sketch of the PSCs is shown in Figure 4a, while in 4b is reported the corresponding energy level diagram.[22]

The solar cell including the $CsSn_{0.5}Ge_{0.5}I_3$ perovskite showed a PCE of 7.11% achieved with open-circuit voltage (V_{OC}) of 0.63 V and a fill factor (FF) of 0.606 and a quite stable performance up to 500 h under nitrogen atmosphere.[22]

The results of this paper may guide future directions in the stabilization of easily oxidized cations other than Ge^{2+} through the exploitation of native-oxide approach. Further research is needed in order to tailor and rationalize such a promising approach.

Notably, the alloying strategy has been used to improve the air-stability of PSCs by Ito and co-workers by preparing a series of samples in the mixed systems $FA_{0.75}MA_{0.25}Sn_{1-x}Ge_xI_3$ ($x = 0$, 0.05, 0.1, and 0.2).[23] After a full characterization of the structural, optical, electronic, and morphological properties of thin films of the mixed Sn–Ge compositions, the authors

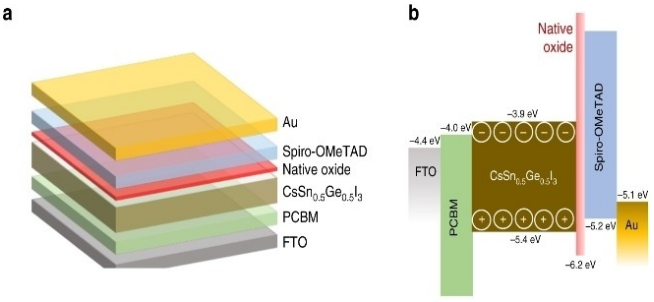

Figure 4. a) PSC structure with $CsSn_{0.5}Ge_{0.5}I_3$ b) diagram of the energy levels. Reproduced from reference [22] with permission from Springer Nature.

prepared devices on ITO substrates coated with PEDOT:PSS. Figure 5a reports the *J-V* curves of the best performing devices for each composition, showing that at 5 wt% doping of Ge, the J_{SC} increased to 19.80 mA/cm^2 and FF improved to 0.55, with an overall efficiency of 4.48%.[23] Further increase of the Ge-doping leads to a general decrease of all photovoltaic parameters which is correlated to the progressive reduction of UV-vis absorption. Figure 5b demonstrates that, at $x=0.05$, the PSC exhibited a superior stability in air with a retention of about 80% of its original efficiency after 60 min to be compared to about 10% for the $x=0$ PSC.[23] This effect was attributed to the surface passivation effect of Sn induced by Ge which reduces the probability of the Sn^{2+} to be oxidized into Sn^{4+}. While the passivation effect of Ge is sound, further investigation on this aspect should be performed to confirm this feature which could be of interest for further development of stable Ge-based PSCs.

On the same alloyed perovskite, namely $FA_{0.75}MA_{0.25}Sn_{1-x}Ge_xI_3$, the impact of SnF_2 and GeI_2 additives has been investigated to reduce the oxidation tendency of Sn^{2+} as well as the trap density.[24] As already observed on pure tin-based metal halide perovskites, the addition of SnF_2 confirmed its positive role in reducing the molar ratio of Sn^{4+}, as determined by XPS.[24,25] On the other hand, the incorporation of 5 mol% of GeI_2, resulted in a significant reduction of the trap density which has been correlated to the possible Sn vacancy filling by the smaller Ge atoms.[24] Thanks to the simultaneous presence of these additives, the authors improved the photovoltaic performance of the prepared solar cells achieving an efficiency around 7.9%.[24]

The space left for further investigation of alloyed systems to produce more efficient PSCs and improve/control the stability of the perovskite layers is significant. The passivation/additives strategies reported above merit to be systematically explored in detail since the proved to be effective in tin-based PCSs to improve stability.

Just to conclude this section, we may highlight the extended prediction of lead-free mixed tin and germanium halide perovskite materials by Ju *et al.*[21] The reader is referred to ref. 21 for further details, while in Figure 6 is shown the plot of the calculated band gaps for the series of predicted mixed samples.[21]

Calculations predict small effective masses and low exciton-binding energies together with a highly tunable band gap

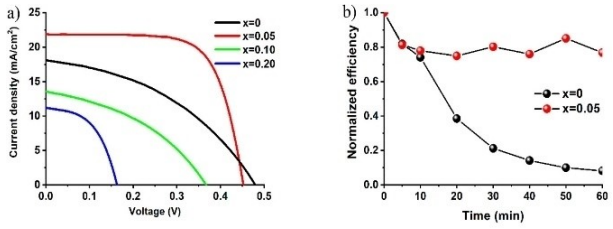

Figure 5. (a) *J-V* curve of the devices measured at room temperature under 1 sun illumination in air without encapsulation using a 0.10 cm^2 mask. (b) Normalized efficiency vs time (stability test) of $x=0$ and $x=0.05$ solar cells. Reproduced from reference [23] with permission from the American Chemical Society.

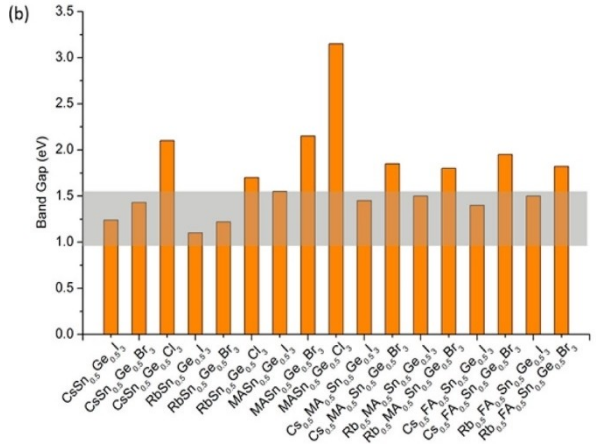

Figure 6. Calculated band gaps for a series of perovskites with favorable Goldschmidt's tolerance factors (see ref. 21 for details). Light-gray horizontal bar defines the range of optimal band gaps for solar-cell materials. Reproduced from reference [21] with permission from the American Chemical Society.

spanning a range from about 0.90 to 3.15 eV as a function of the compositional variation involved in the mixing element strategy.[21] To date, few of them have been synthesized, characterized and tested in devices, therefore we expect and hope for further efforts in this direction by experimentalists.

All-inorganic $CsGeX_3$ (X=Cl, Br, I) have been as well object of some experimental and several computational works. The first elucidation of the crystal structure of these phases and their phase transition dates back to 1987.[26] $CsGeCl_3$ possesses the classical cubic perovskite unit cell, while $CsGeBr_3$ and $CsGeI_3$ display a rhombohedral distortion caused by a second-order Jahn-Teller effect.[26–29] Computational modelling reveals that $CsGeX_3$ halide perovskites have a direct band gap, which can be tuned from ~1.6 eV ($CsGeI_3$) to ~3.7 eV ($CsGeCl_3$), showing therefore values very close to those of the analogous Pb-containing perovskites.[30,31] Further studies highlighted strong absorption coefficients, large dielectric constants, small effective masses, non-linear optical behavior, strong ferroelectric polarization, and even ultralow thermal conductivities of interest for thermoelectric applications.[16,17,32–34] Despite this significant amount of computational and theoretical work on $CsGeX_3$ (X=Cl, Br, I) perovskites, few experimental works have been reported in the current literature. $CsGeI_3$ was first reported by Stoumpos and co-workers with a measured band gap of about 1.6 eV.[5] Later, PCSs containing $CsGeI_3$ as active layer were prepared providing a low PCE around 0.11%.[13] $CsGeX_3$ (X=Cl, Br) perovskites were investigated by Schwarz and co-workers also highlighting the effect of the application of high-pressure on the structural and electronic properties.[29,35] Quite impressively, the band gap of both perovskites has an extremely large reduction (red-shift) by increasing pressure with a rate, for $CsGeBr_3$, of −0.61 eV/GPa.[36] An analogous behavior has been observed in Sn-based perovskites, while for Pb analogues the impact of high-pressure on the band gap is usually smaller.[37–39]

$CsGeBr_3$ has been proposed as an infrared nonlinear optical crystal by Tang and co-workers.[40] By second-harmonic gener-

ation measurements, this compositions showed a nonlinear optical efficiency 1.62 times larger than that of $CsGeCl_3$. From this accurate investigation, $CsGeBr_3$ is proposed as a potential useful material for nonlinear optics application in the infrared region.[40]

Recently, $CsGeX_3$ (X=Cl, Br) perovskites nanocrystals have been reported by Men and co-workers.[27] By applying a common synthetic procedure, with the addition of cysteammonium halides, crystals of the order of 25–30 nm have been obtained. Figure 7 reports some representative images of $CsGeI_3$ and $CsGeBr_3$ nanocrystals.

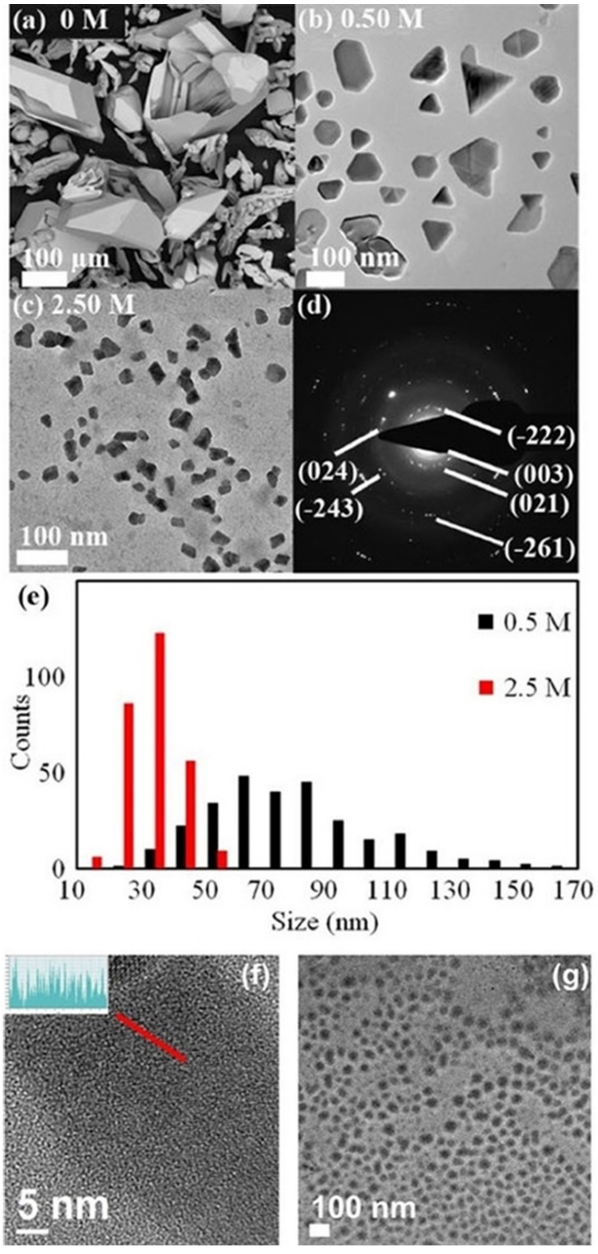

Figure 7. SEM (a), TEM (b–c), SAED (d) and size distribution histograms (e) for $CsGeI_3$ prepared with [cysteNH$_3$X] = 0.5 M. HRTEM image (f) of a $CsGeI_3$ nanocrystal displaying lattice fringes along the (021) direction and (g) TEM images of $CsGeBr_3$ synthesized with [cysteNH$_3$X] = 3.33 M. Reproduced from reference [27] with permission from Wiley-VCH.

According to the authors, part of the cysteammonium halide enters the structure as cysteNH$_3^+$ cation, leading to a slight cell expansion and band gap increase.[27] Finally, Mn^{2+} was successfully incorporated into the $CsGeX_3$ (X=Cl, Br) perovskites up to 29% in bulk and 16% in nanocrystalline samples with a limited effect on the optical properties.

Overall, the experimental works available on bulk, nanocrystals, and thin films of $CsGeX_3$ (X=Cl, Br) perovskites is still very scarce, and it is desirable that such gap is filled soon to gain a better understanding of their basic properties, stability, and film formation.

2.2. Low-dimensional perovskites

Together with 3D metal halide perovskite, some limited research efforts were directed towards low-dimensional perovskites, namely 0D and 2D systems.

Chang and co-workers investigated the Ruddlesden-Popper series $BA_2MA_{n-1}Ge_nBr_{3n+1}$ derived by layering the parent 3D perovskite $MAGeBr_3$ (with butylammonium BA=$CH_3(CH_2)_3NH_3^+$ and methylammonium MA=$CH_3NH_3^+$).[41] Analogously to the Pb-counterparts, the crystal structure of these materials consist of the stacking of n inorganic perovskite layers, intercalated with bulky butylammonium cations acting as spacers. The authors focused on the $n=1$ and 2 of this series with the aim of highlighting the quantum confinement effects and comparing their properties with $MAGeBr_3$. Figure 8 reports the optical properties of the synthetized materials showing the reflectance and PL spectra for $n=1$, 2, and ∞ (3D) compounds.[41]

The band gaps extracted from the Tauc plots of absorption demonstrate a progressive blue-shift moving from $MAGeBr_3$ (2.85 eV) to BA_2GeBr_4 (2.95 eV), and to $BA_2MAGe_2Br_7$ (2.98 eV), as expected from increased quantum confinement of optical excitations within the layers by reducing n.[41] Photoluminescence decays in time-resolved measurements, demonstrated similar initial decay time for all the samples as possibly due to

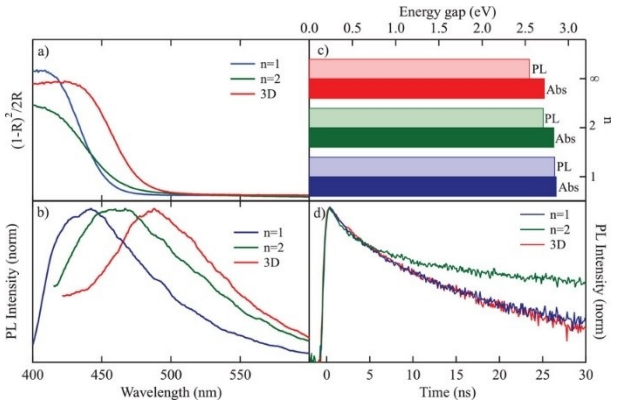

Figure 8. a) Absorption and b) PL spectra of the $BA_2MA_{n-1}Ge_nBr_{3n+1}$ compounds (for n = 1, 2, ∞) as a function of wavelength at room temperature. c) Band gaps for the same compounds (extracted from the Tauc plot) compared to PL peak energy. d) PL decay time of the $BA_2MA_{n-1}Ge_nBr_{3n+1}$ compounds (for n = 1, 2, ∞) at room temperature. Reproduced from reference [41] with permission from Wiley-VCH.

nonradiative recombination through defects. Through DFT calculations of the electronic structure, the authors attributed the weak dependance of band gap from quantum confinement to the peculiar nature of the germanium orbitals, leading to band structure of layered RP germanium bromide perovskites similar to the parent 3D perovskite, differently to the case of analogous lead-based compounds.[41]

The PEA_2GeI_4 ($PEA{=}C_6H_5(CH_2)_2NH_3^+$) 2D perovskite has been reported by Cheng an co-workers as one of the first examples of layered iodide Ge-based perovskite.[42] This compounds crystallizes in a triclinic crystal system (space group *P*1) with organic PEA^+ cations intercalated as spacers between the $[GeI_6]^{4-}$ octahedral planes. A sketch of the crystal structure is reported in Figure 9a.

The band gap of PEA_2GeI_4 was measured to be 2.12 eV and DFT calculation confirmed that Ge^{2+} cation mainly contributes to the bottom of the conduction band while the contribution of the I^- anion is mainly concentrated on top of the valence band.[42] PL measurements show a wide peak centered at 630 nm and, from the decay curves, a short-lifetime of 408 ps and a long-lifetime of 1.28 ns were determined. In this work the authors performed one of the few stability tests available for Ge-based perovskite by comparing $MAGeI_3$ and PEA_2GeI_4 powders exposed to a relative humidity level of 60% at 25 °C. After 2 days storing in the humidity environment, $MAGeI_3$ showed evident MAI and GeI_4 diffraction peaks in the patterns due to the decomposition and oxidation processes (see Figure 9b).[42] On the other hand, the pattern of PEA_2GeI_4 remained almost unchanged: this result comes from the hydrophobic nature of PEA cations avoiding the direct contact of water with perovskite, thus delaying the moisture degradation and the subsequent oxidation (see Figure 9c).[42]

The same authors further investigated the mixed Sn–Ge $PEA_2Ge_{1-x}Sn_xI_4$ system ($x = 0$, 0.125, 0.25, 0.5).[43] As could be anticipated, the progressive Sn doping leads to a linear red-shift of the band gap from 2.13 to 1.95 eV in accordance with the Vegard's law, as shown in Figure 10. The PL spectra of $PEA_2Ge_{1-x}Sn_xI_4$ perovskites show emission peaks at wavelengths of 613 ($x = 0$), 628 ($x = 0.125$), 642 ($x = 0.25$), and 655 ($x = 0.5$) nm with a decrease in full width at half-maximum by increasing the Sn content.[43] While the extension of the alloying was limited to this concentration range (up to $x = 0.5$), it should be expected a

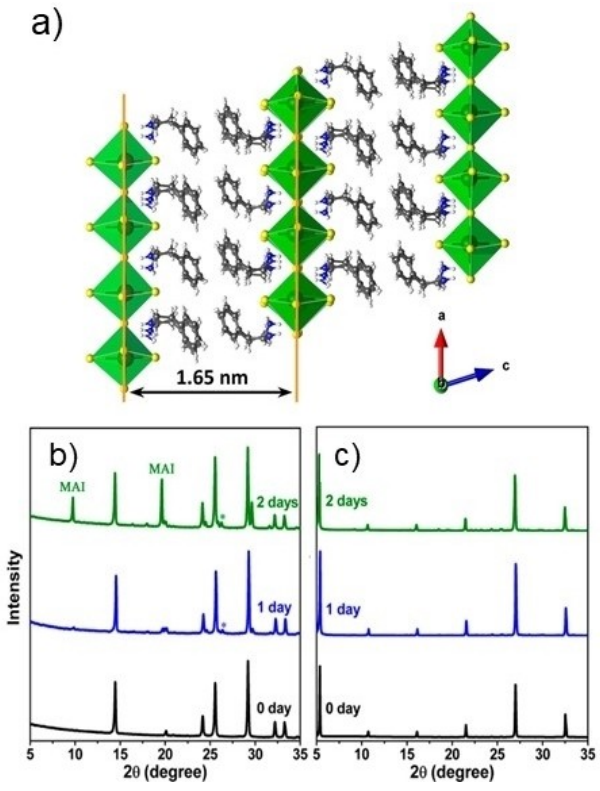

Figure 9. a) Sketch of the crystal structure of PEA_2GeI_4, viewed along the *b* axis. Violet, yellow, gray, blue, and white spheres represent Ge, I, C, N, and H atoms, respectively. PXRD of $MAGeI_3$ (b) and $(PEA)_2GeI_4$ (c), exposed to 60% relative humidity at 25 °C for different time intervals. Asterisks denote signals from GeI_4. Reproduced from reference [42] with permission from the American Chemical Society.

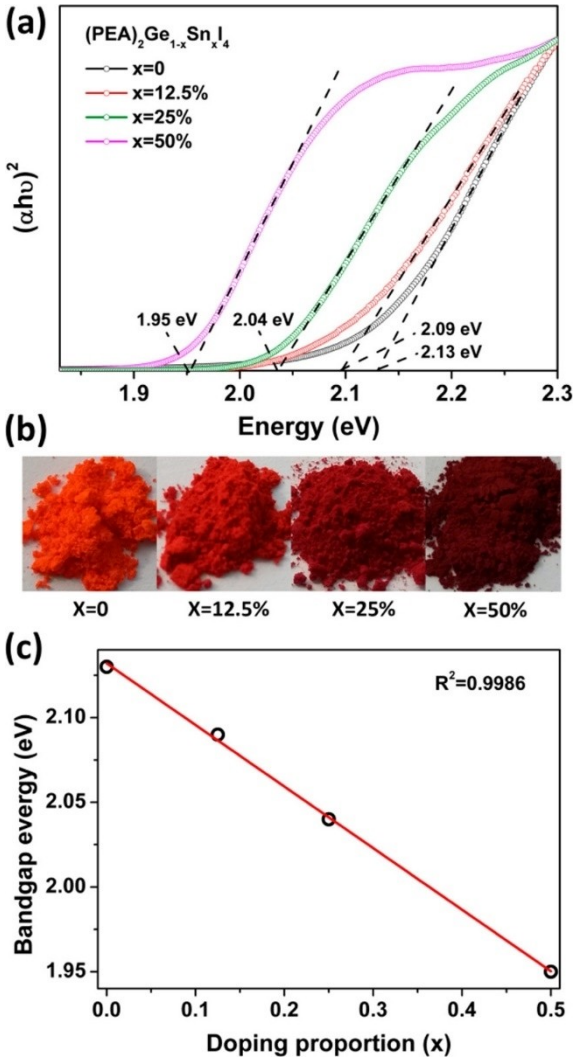

Figure 10. (a) Tauc plots vs. energy of $(PEA)_2Ge_{1-x}Sn_xI_4$ ($x = 0$, 0.125, 0.25, 0.5). (b) Photos of the compounds with different Sn content. (c) Trend of band gap as a function of tin doping (*x*). Reproduced from reference [43] with permission from the American Chemical Society.

complete solid-solubility between Ge and Sn on the crystal structure.

Finally, thermogravimetric analysis (TGA) was used to check the thermal behavior of the mixed Ge–Sn perovskites demonstrating high stability up to 250 °C, i.e. a suitable range for device operation.[43]

Some further computational work explored other Ruddlesden-Popper Ge-containing perovskites such as the $BA_2MA_{n-1}Ge_nI_{3n+1}$ (n = 2–4) system.[44] By DFT calculations, the trend of electronic and optical properties was predicted showing a band gap decrease from 2.35 eV to 2.29 eV for Ge-based 2D perovskites by increasing the layer thickness from n = 1 to 4 with also a reduction of exciton binding energies and light absorption improvement with increasing layer thickness.[44] Such computational data provide an indication that Ge-based 2D perovskites may be suitable lead-free candidates to be incorporated in photovoltaic and/or photoelectronic devices providing reasonable performance, lower environmental concerns and enhanced device longevity.[44] To date, the number of experimental reports on two-dimensional Ge-containing MHPs is very limited but they appear to be, also based on the intrinsic distortion observed in the GeX_6 octahedra, good candidates for broadband emitting materials. For example, possible future experimental efforts could couple organic spacers such as 2,2′-(ethylenedioxy)bis(ethylammonium) (EDBE) which are known to induce strong octahedral distortion to further extend the emission spectra of 2D perovskites possibly achieving white emitting materials. The lesson learned by two dimensional Pb- and Sn-perovskites, which show an impressive properties tunability induced by spacer cation, should be extended to germanium-containing materials to overcome the toxicity issue of Pb-based materials and to unveil novel properties related to crystal distortion effects.[45] Moreover, 0D and 1D Ge-based materials appear to be a nearly completely unexplored research field which should considered in the future.

3. Summary and Outlook

In this Minireview we attempted to provide a concise overview of the state-of-the-art experimental and computational research on Ge-based metal halide perovskites. Struggling with the toxicity issues of lead-containing systems, researchers on MHPs are now significantly enlarging the panorama of possible metals (e.g., Sn, Bi, Sb, Ge), with Sn as the major player in this novel sustainable future for PSCs.[2,46] Ge-containing perovskites still deserve a deep investigation starting from the basic science point of view to further exploit their possible functionalities which could extend to a rich range of fields, in analogy with Pb- and Sn-based systems. While sharing with tin some issues related to cation oxidation, Ge^{2+} appears to be more stable, and a proper materials chemistry design based on metal alloying and organic cation tailoring could improve the stability of germanium halide perovskites. Other issues to overcome, shared with Bi- and Sb-perovskites, are the poor solubilities in common polar organic solvents of germanium precursors, but the advancement in the field of physical vapor deposition of MHPs could provide the required answer.[47] Exploration of lower-dimensional systems is still at infancy and the exciting results accumulated in the last years on tin and lead analogues should trigger a significant amount of experimental and computational research to unveil the structure-property correlations in these systems. Lower-dimensional Ge-based perovskites in addition to RP materials still call for a significant experimental and computational investigation to highlight the role of spacer cation, structural distortion, alloying and quantum confinement on optical properties. Another strategy that could be explored for Ge-based materials is the preparation of perovskite derivative materials including Ge^{4+} cations, thus getting rid of the oxidation issues. This approach has been successfully applied for Sn-based perovskites where Cs_2SnX_6 vacancy-ordered inorganic double perovskite proved to be promising phases for photovoltaics and optoelectronic properties.[48,49] To date, only the computational investigation of possible Ge-based vacancy ordered perovskites has been accomplished and urgent experimental effort should be directed in this way.[50]

To summarize, future urgent prospects on Ge-based MHPs where experimental and computational work could be directed are:

i) exploration and extension of the compositional range of 3D and low-dimensional perovskites making use of the knowledge and understanding achieved on Pb- and Sn-based systems;
ii) improvement of the understanding of the stability issues (particularly of oxidation tendency) and exploring the possible application of the routes used for Sn-based materials;
iii) design of tailored cells architectures/materials for devices containing germanium halide perovskites;
iv) exploration of applicative fields where preliminary encouraging results have been achieved such as nonlinear optics.

While the possible application of germanium halide perovskites in photovoltaics seems, to date, hard to be competitive in terms of performance also with respect to tin analogues, it appears that interesting optoelectronic properties could be instead uncovered in this family. To conclude, germanium was a late discovered element in the history of chemistry (1886) and the same is happening relative to its potential in the field of MHPs but we expect to see an increasing and growing interest in the forthcoming years with unexpected and exciting avenues for possible applications.

Conflict of Interest

The authors declare no conflict of interest.

Keywords: crystal structures · germanium · lead-free perovskites · metal halide perovskites · solar cells

[1] J. Y. Kim, J.-W. Lee, H. S. Jung, H. Shin, N.-G. Park, *Chem. Rev.* **2020**, *120*, 7867.
[2] A. Abate, *Joule* **2017**, *1*, 659.

[3] J. Cao, F. Yan, *Energy Environ. Sci.* **2021**, *14*, 1286.
[4] L. Liang, P. Gao, *Adv. Sci.* **2018**, *5*, 1700331.
[5] C. C. Stoumpos, L. Frazer, D. J. Clark, Y. S. Kim, S. H. Rhim, A. J. Freeman, J. B. Ketterson, J. I. Jang, M. G. Kanatzidis, *J. Am. Chem. Soc.* **2015**, *137*, 6804.
[6] A. Mancini, P. Quadrelli, G. Amoroso, C. Milanese, M. Boiocchi, A. Sironi, M. Patrini, G. Guizzetti, L. Malavasi, *J. Solid State Chem.* **2016**, *240*, 55.
[7] Y. Dang, X. Liu, B. Cao, X. Tao, *Matter* **2021**, *4*, 794.
[8] S. Yue, S. C. McGuire, H. Yan, Y. S. Chu, M. Cotlet, X. Tong, S. S. Wong, *ACS Omega* **2019**, *4*, 18219.
[9] A. Pisanu, C. Ferrara, P. Quadrelli, G. Guizzetti, M. Patrini, C. Milanese, C. Tealdi, L. Malavasi, *J. Phys. Chem. C* **2017**, *121*, 8746.
[10] A. Bernasconi, L. Malavasi, *ACS Energy Lett.* **2017**, *2*, 863.
[11] A. Bernasconi, K. Page, Z. Dai, L. Z. Tan, A. M. Rappe, L. Malavasi, *J. Phys. Chem. C* **2018**, *122*, 28265.
[12] K. Page, J. E. Siewenie, P. Quadrelli, L. Malavasi, *Angew. Chem. Int. Ed.* **2016**, *55*, 14320.
[13] T. Krishnamoorthy, H. Ding, C. Yan, W. L. Leong, T. Baikie, Z. Zhang, M. Sherburne, S. Li, M. Asta, N. Mathews, S. G. Mhaisalkar, *J. Mater. Chem. A* **2015**, *3*, 23829.
[14] I. Kopacic, B. Friesenbichler, S. F. Hoefler, B. Kunert, H. Plank, T. Rath, G. Trimmel, *ACS Appl. Mater. Interfaces* **2018**, *1*, 343.
[15] J. H. Noh, S. H. Im, J. H. Heo, T. N. Mandal, S. I. Seok, *Nano Lett.* **2013**, *13*, 1764.
[16] P.-P. Sun, Q.-S. Li, L.-N. Yang, Z.-S. Li, *Nanoscale* **2016**, *8*, 1503.
[17] Y.-Q. Zhao, B. Liu, Z.-L. Yu, J. Ma, Q. Wan, P. He, M.-Q. Cai, *J. Mater. Chem. C* **2017**, *5*, 5356.
[18] D. Umadevi, G. W. Watson, *ACS Omega* **2019**, *4*, 5661.
[19] A.-A. Kanoun, M. B. Kanoun, A. E. Merad, S. Goumri-Said, *Sol. Energy* **2019**, *182*, 237.
[20] S. Nagane, D. Ghosh, R. L. Z. Hoye, B. Zhao, S. Ahmad, A. B. Walker, M. S. Islam, S. Ogale, A. Sadhanala, *J. Phys. Chem. C* **2018**, *122*, 5940.
[21] M.-G. Ju, J. Dai, L. Ma, X. C. Zeng, *J. Am. Chem. Soc.* **2017**, *139*, 8038.
[22] M. Chen, M.-G. Ju, H. F. Garces, A. D. Carl, L. K. Ono, Z. Hawash, Y. Zhang, T. Shen, Y. Qi, R. L. Grimm, D. Pacifici, X. C. Zeng, Y. Zhou, N. P. Padture, *Nat. Commun.* **2019**, *10*, 16.
[23] N. Ito, M. A. Kamarudin, D. Hirotani, Y. Zhang, Q. Shen, Y. Ogomi, S. Iikubo, T. Minemoto, K. Yoshino, S. Hayase, *J. Phys. Chem. Lett.* **2018**, *9*, 1682.
[24] C. H. Ng, K. Nishimura, N. Ito, K. Hamada, D. Hirotani, Z. Wang, F. Yang, S. Iikubo, Q. Shen, K. Yoshino, T. Minemoto, S. Hayase, *Nano Energy* **2019**, *58*, 130.
[25] T. M. Koh, T. Krishnamoorthy, N. Yantara, C. Shi, W. L. Leong, P. P. Boix, A. C. Grimsdale, S. G. Mhaisalkar, N. Mathews, *J. Mater. Chem. A* **2015**, *3*, 14996.
[26] G. Thiele, H. W. Rotter, K. D. Schmidt, *Z. Anorg. Allg. Chem.* **1987**, *545*, 148.
[27] L. Men, B. A. Rosales, N. E. Gentry, S. D. Cady, J. Vela, *ChemNanoMat* **2019**, *5*, 334.
[28] M. G. Goesten, R. Hoffmann, *J. Am. Chem. Soc.* **2018**, *140*, 12996.
[29] D.-K. Seo, N. Gupta, M.-H. Whangbo, H. Hillebrecht, G. Thiele, *Inorg. Chem.* **1998**, *37*, 407.
[30] L. Jiang, T. Wu, L. Sun, Y.-J. Li, A.-L. Li, R.-F. Lu, K. Zou, W.-Q. Deng, *J. Phys. Chem. C* **2017**, *121*, 24359.
[31] D. Ray, C. Clark, H. Q. Pham, J. Borycz, R. J. Holmes, E. S. Aydil, L. Gagliardi, *J. Phys. Chem. C* **2018**, *122*, 7838.
[32] W. Ming, H. Shi, M.-H. Du, *J. Mater. Chem. A* **2016**, *4*, 13852.
[33] L.-C. Tang, Y.-C. Chang, J.-Y. Huang, M.-H. Lee, C.-S. Chang, *Jpn. J. Appl. Phys.* **2009**, *48*, 112402.
[34] U.-G. Jong, C.-J. Yu, Y.-H. Kye, S.-N. Hong, H.-G. Kim, *Phys. Rev. Mater.* **2020**, *4*, 075403.
[35] D. Liu, Q. Li, H. Jing, K. Wu, *RSC Adv.* **2019**, *9*, 3279.
[36] U. Schwarz, F. Wagner, K. Syassen, H. Hillebrecht, *Phys. Rev. B* **1996**, *53*, 12545.
[37] M. Coduri, T. B. Shiell, T. A. Strobel, A. Mahata, F. Cova, E. Mosconi, F. De Angelis, L. Malavasi, *Mater. Adv.* **2020**, *1*, 2840.
[38] M. Coduri, T. A. Strobel, M. Szafrański, A. Katrusiak, A. Mahata, F. Cova, S. Bonomi, E. Mosconi, F. De Angelis, L. Malavasi, *J. Phys. Chem. Lett.* **2019**, *10*, 7398.
[39] P. Postorino, L. Malavasi, *J. Phys. Chem. Lett.* **2017**, *8*, 2613.
[40] L. C. Tang, J. Y. Huang, C. S. Chang, M. H. Lee, L. Q. Liu, *J. Phys. Condens. Matter* **2005**, *17*, 7275.
[41] X. Chang, D. Marongiu, V. Sarritzu, N. Sestu, Q. Wang, S. Lai, A. Mattoni, A. Filippetti, F. Congiu, A. G. Lehmann, F. Quochi, M. Saba, A. Mura, G. Bongiovanni, *Adv. Funct. Mater.* **2019**, *29*, 1903528.
[42] P. Cheng, T. Wu, J. Zhang, Y. Li, J. Liu, L. Jiang, X. Mao, R.-F. Lu, W.-Q. Deng, K. Han, *J. Phys. Chem. Lett.* **2017**, *8*, 4402.
[43] P. Cheng, T. Wu, J. Liu, W.-Q. Deng, K. Han, *J. Phys. Chem. Lett.* **2018**, *9*, 2518.
[44] L. Ma, M.-G. Ju, J. Dai, X. C. Zeng, *Nanoscale* **2018**, *10*, 11314.
[45] X. Li, J. M. Hoffman, M. G. Kanatzidis, *Chem. Rev.* **2021**, *121*, 2230.
[46] F. De Angelis, *ACS Energy Lett.* **2021**, *6*, 1586.
[47] S. Bonomi, L. Malavasi, *J. Vac. Sci. Technol. A* **2020**, *38*, 060803.
[48] Y. Cai, W. Xie, H. Ding, Y. Chen, K. Thirumal, L. H. Wong, N. Mathews, S. G. Mhaisalkar, M. Sherburne, M. Asta, *Chem. Mater.* **2017**, *29*, 7740.
[49] A. Veronese, M. Patrini, D. Bajoni, C. Ciarrocchi, P. Quadrelli, L. Malavasi, *Front. Chem.* **2020**, *8*, 35.
[50] D. Liu, L. Liang, R. Sa, *Chem. Phys.* **2021**, *542*, 111075.

Manuscript received: April 26, 2021
Revised manuscript received: May 25, 2021
Accepted manuscript online: May 26, 2021